Creep Anisotropy of Zircaloy-2 Cladding during Irradiation

S. H. SHANN, L. F. Van SWAM
Advanced Nuclear Fuels Corporation, Richland, WA USA

ABSTRACT

A procedure is described to determine the axial/radial and circumferential/radial contractile strain ratios (the R and P factors in the Von Mises-Hill flow relations) from post-irradiation dimensional measurements of Zircaloy-2 of BWR fuel rods, tie rods and water rods. Values for R and P have been determined for textured cold-worked stress-relieved (CWSR) Zircaloy-2 cladding made to Advanced Nuclear Fuels Corp. (ANF) specifications. A sensitivity study was performed to evaluate the effects of measurement uncertainties on the derived values of R and P and on the engineering application of the model to predict the in-reactor deformation of CWSR Zircaloy-2 cladding.

1 INTRODUCTION

The cold-worked stress-relieved Zircaloy-2 tubing used by Advanced Nuclear Fuels Corporation (ANF) in the fabrication of nuclear fuel rods for boiling water reactors (BWRs) is strongly textured. The majority of the basal poles lie in the radial - circumferential (transverse) plane of the tubing with the highest concentration of basal poles at plus and minus 30° from the radial direction. The hexagonal close packed crystalline structure of the textured tubing causes anisotropic mechanical deformation behavior. This anisotropic behavior is most readily modelled by using axial/radial and circumferential/radial contractile strain ratios, the R and P factors, in the von Mises-Hill flow relations. This paper describes a procedure to determine the R and P factors for irradiation induced creep of stress-relieved Zircaloy-2 cladding as determined from deformation measurements on irradiated BWR assemblies and fuel rods.

2 MODEL DESCRIPTION

The creep correlation for textured anisotropic zircaloy can be expressed by the following equations (Murty and Adams):

$$\sigma_g^2 = \frac{R(\sigma_r - \sigma_\theta)^2 + RP(\sigma_\theta - \sigma_z)^2 + P(\sigma_z - \sigma_r)^2}{P(R + 1)} \qquad (1)$$

$$\begin{bmatrix} \dot{\epsilon}_r \\ \dot{\epsilon}_\theta \\ \dot{\epsilon}_z \end{bmatrix} = \frac{\dot{\epsilon}_g}{P(R+1)\sigma_g} \cdot \begin{bmatrix} (R+P) & -R & -P \\ -R & R(P+1) & -RP \\ -P & -RP & P(R+1) \end{bmatrix} \begin{bmatrix} \sigma_r \\ \sigma_\theta \\ \sigma_z \end{bmatrix} \quad (2)$$

Before the onset of pellet-cladding interaction the state of stress in the cladding does not change significantly during irradiation. Thus the above strain rate equation can be integrated and written as:

$$\begin{bmatrix} \epsilon_r \\ \epsilon_\theta \\ \epsilon_z \end{bmatrix} = \frac{\epsilon_g}{P(R+1)\sigma_g} \cdot \begin{bmatrix} (R+P) & -R & -P \\ -R & R(P+1) & -RP \\ -P & -RP & P(R+1) \end{bmatrix} \begin{bmatrix} \sigma_r \\ \sigma_\theta \\ \sigma_z \end{bmatrix} \quad (3)$$

where σ_r, σ_θ, & σ_z = radial, circumferential, & axial stress
ϵ_r, ϵ_θ, & ϵ_z = stress-induced radial, circumferential, & axial strain
σ_g and ϵ_g = generalized stress and strain
R and P = axial/radial and circumferential/radial contractile strain ratios

For an engineering application of the model to predict strains in tubing under a given stress condition, the contractile strain ratios, R and P, need to be derived from post-irradiation deformation measurements on tubing.

It is generally assumed that the in-reactor stress induced strain has two components, thermal and irradiation creep strain (Gittus, et al). The correlation given by Gittus indicates that, at typical reactor operating temperatures (280 - 320°C), the irradiation induced creep strain is much larger than the thermal creep strain. The irradiation creep strain has been determined to have the following stress dependence:

$$\epsilon \propto \sigma^{1.23} \quad (4)$$

In addition to the stress induced strains, cold-worked stress-relieved Zircaloy-2 tubing undergoes stress-free neutron irradiation-induced growth (length increase) in the axial direction of the tubing. In single crystals of zircaloy the irradiation-induced stress free growth is due to the formation of interstitial loops on prism planes and vacancy loops on basal planes (Franklin et al). In textured Zircaloy-2, with the majority of the basal poles at 30° to the radial direction, axial elongation and radial contraction take place with an insignificant change in the circumferential direction.

3 EXPERIMENTAL

A boiling water reactor fuel element consists of a square array of fuel rods with an upper and a lower tieplate fitting. The upper and lower endcaps of the fuel rods have long shanks which are captured in the upper and lower tieplates. This arrangement is shown in Figure 1. Each BWR fuel element contains 3 different kinds of rods that are stressed differently.

a Standard fuel rods have non-threaded upper and lower endcap shanks. A small Inconel holddown spring is placed on the upper endcap to maintain a downward force on the fuel rod and keep the rod seated in the lower tieplate. The force of the fuel rod internal plenum spring which produces a tensile stress in the longitudinal direction of the cladding is approximately counter balanced by the compressive stress of the fuel rod holddown spring. During operation, therefore, and under the influence of the coolant and rod internal pressure, the cladding in a standard fuel rod is, as long as no hard pellet-to-clad interaction takes place, subjected to a biaxial state of stress with a ratio of hoop to axial stress of 2 to 1.

b Water rods do not contain fuel. Small holes are drilled in the cladding near the bottom and the top of the rods to allow the passage of water through the rods. During operation the pressure inside the water rods is equal to the system pressure. The Inconel holddown spring on top of the water rod exerts a very small compressive force on the cladding. For the analysis carried out here this axial stress may be neglected, and the cladding in a water rod can be considered to be free of stress.

c Tie rods are special fuel rods that have a lower endcap which is threaded into the lower tieplate and an upper endcap locking mechanism that holds the upper tieplate in place. The upper and lower tieplate are forced apart by the holddown springs on the fuel rods and water rods. The tie rods, as their name implies, hold the upper and lower tieplate together. Eight tie rods are typically used in a 9x9 BWR design and each tie rod carries a tensile load equal to one-eighth of the compressive force of the 73 holddown springs. At operation the tie rods are under a biaxial state of stress brought on by the coolant system pressure, the axial tensile force of the rod plenum spring and the axial tensile force of the holddown springs on the other fuel rods. The hoop to axial stress ratio will, therefore, be greater than 2.

After irradiation of the fuel for different lengths of time, two types of measurements have been made. Rods diameter measurements were made to determine the diametral rod creep-down, and rod length measurements were made to determine rod length changes. The rod diametral deformation is made up of two components: stress-induced thermal creep strain and stress-induced irradiation creep. There are 3 components in the measured rod length (axial deformation) changes: stress-induced thermal creep, stress-induced irradiation creep and stress-free irradiation-induced growth.

4 THEORETICAL DEVELOPMENT

4.1 Model Assumptions

To apply the model described in Section 2 to fuel rods before the onset of Pellet-Cladding Interaction and to determine the values of R and P, the following assumptions were made:

1. The thermal creep strain component in the post-irradiation measured deformation data can be neglected.
2. Contractile strain ratios of stress-induced irradiation creep strain do not change during irradiation.
3. Tie rods and standard fuel rods in a given fuel assembly experience an identical hoop stress.
4. The compressive holddown spring force and the tensile plenum spring force on standard fuel rods cancel one another.
5. Thin wall tubing approximation applies.

The first assumption is supported by Gittus's paper: for stress-induced strain, thermal creep strain is minor in comparison with irradiation creep strain at the operating temperatures considered. The second assumption simplifies the calculation procedure and, since it may be assumed that the deformation mechanisms do not change, is justified for an engineering application of the model. Without pellet-to-cladding interaction, which is the case early in life, all fuel rods have an identical hoop stress, making the third assumption applicable. For the fourth assumption, calculations were performed, and the results indicated that stress due to compression spring force and plenum spring force on standard fuel rods nearly cancel one another, and the sum of these stresses is very small in comparison with the stress caused by the coolant pressure. Any errors induced by neglecting the spring

forces on the fuel rod are insignificant. The ratio cladding wall thickness to cladding diameter is typically on the order of 7 percent or less. Hence, for current design fuel rods, a thin wall tubing approximation is applicable.

4.2 Calculation of Irradiation Induced Growth

As indicated in Section 3, the water rod cladding is nearly free of stress during operation. Hence, measured length increases of water rods in each assembly were used to determine the stress-free neutron irradiation-induced growth of the stress-relieved Zircaloy-2 cladding in the same assembly.

4.3 Calculation of Axial to Circumferential Strain Ratio for Fuel Rods

The measured rod length change of standard fuel rods minus the stress-free irradiation-induced component (determined through water rod growth measurements as described in Section 4.2) gives the stress-induced creep component.

The cladding in standard fuel rods is closed on both ends. Under thin wall approximation and Assumption 4 of Section 4.1, $\sigma_r = 0$ and $\sigma_\theta = 2\,\sigma_z$, the following equation is derived from Equation 2:

$$\frac{\epsilon_z}{\epsilon_\theta} = \frac{1-R}{R}\,\frac{P}{2+P} \tag{5}$$

The stress-induced ratio $\epsilon_z/\epsilon_\theta$ can be determined from the measured data. The values of R and P cannot be derived from Equation (5) alone. This equation only provides a correlation between R and P. As is obvious from Equation (5) and shown in Figure 2, for a given ratio of $\epsilon_z/\epsilon_\theta$ the value of P is fixed for a given R and vice versa.

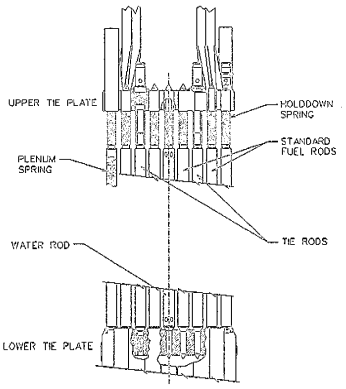

Figure 1 Features of a typical BWR fuel element

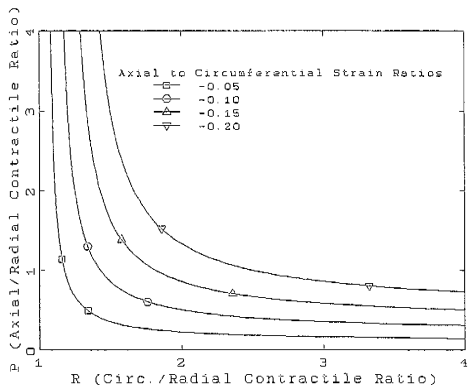

Figure 2 Contractile strain ratios for various strain ratios

4.4 Calculation of Contractile Strain Ratios

The stress-induced axial deformation of tie rods was obtained after subtracting the stress-free irradiation induced growth from the measured total length change. The tie rods and standard fuel rods operate at different hoop to axial stress ratios as a result of the superimposed axial tensile stress in the tie rods. Whereas the standard fuel rods operate at a hoop stress to axial stress ratio of approximately 2, the tie rods operate at a stress ratio that is greater than 2. With this ratio set at x ($x = \sigma_\theta/\sigma_z$), the stress-induced tie rod length change can be expressed as:

$$\epsilon_z \propto \frac{\epsilon_g}{\sigma_e}\left(\frac{1-(x-1)\,R}{X(R+1)}\right)\sigma_\theta \tag{6}$$

The generalized stress in the tie rods can then be calculated from Equation (1) assuming that $\sigma_r = 0$:

$$\sigma_g = \left[\frac{PR + R - \frac{2}{x} PR + \frac{PR}{x^2} + \frac{P}{x^2}}{P(R+1)} \sigma_\theta^2 \right]^{1/2} \quad (7)$$

As indicated before (Section 2), $\epsilon_g \propto \sigma_g^{1.23}$. With the provision that the standard fuel rods and the tie rods in a fuel assembly experience similar hoop stress early in life (Assumption 3 of Section 4.1), it follows that:

$$\frac{\epsilon_z \text{ tie rod}}{\epsilon_z \text{ fuel rod}} = \left[\frac{PR + R - \frac{2}{x} PR + \frac{PR}{x^2} + \frac{P}{x^2}}{R + \frac{PR}{4} + \frac{P}{4}} \right]^{0.115} \frac{1-(x-1)R}{1-R} \frac{2}{x} \quad (8)$$

Using Equations (5) and (8) and the measured fuel rod deformations, the R and P values for irradiation induced creep of cold-worked stress-relieved Zircaloy-2 tubing were determined.

5 DATA BASE USED IN CONTRACTILE STRAIN RATIO DETERMINATION

Rod length change data and rod creepdown data on fuel from four BWRs were used to obtain the desired R and P values for the type cladding used. Table 1 summarizes the number of the data analyzed. The axial deformation data had one measured value per rod; multiple diametral deformation data were measured along the rod at various axial locations.

Table 1. Data base used in analysis

	# of data	# of rods measured	# of assemblies measured
Fuel Rod Diametral Deformation Data	1052	167	14
Fuel Rod Axial Deformation Data	167	167	14
Water Rod Axial Deformation Data	11	11	5
Tie Rod Axial Deformation Data	28	28	7

6 RESULTS AND DISCUSSION

6.1 Results of Data Analysis

The measured water, fuel, and tie rod growth data were first statistically analyzed by using Student's t-test to confirm that the available water, fuel, and tie rod growth data were statistically distinguishable. The t-test indicated that the probability for water rod data and fuel rod data to be two different populations was larger than 95%. The probability for fuel rod and tie rod data to be two different populations was larger than 99%.

6.2 Determination of R and P Values for Irradiated Zircaloy-2

The axial stress in the tie rods was determined from holddown spring force measurements on the standard fuel rods. Due to the somewhat different design and irradiation histories, the value of the hoop to axial stress ratio in the tie rods varied from 2.31 to 2.57. Inserting these values and the measured circumferential (diametral) and axial strains of standard fuel and tie rods in Equations (5) and (8), values for R and P were obtained. For cold worked stress-relieved Zircaloy-2 made to ANF specifications and at a measured stress-induced axial to circumferential strain ratio of 0.15, the values for R and P were 1.38 and 2.39, respectively.

6.3 Results of Sensitivity Study

A sensitivity study was performed to evaluate the effects of measured uncertainties on the calculation results. The sensitivity study found several key factors that might induce large changes in the calculation results. The uncertainty in water rod growth data had the largest effect, and the uncertainty in compression spring force measurements had the second largest effect.

Although the measurement uncertainties cause changes in the R and P values, it was indicated that the error in predictions was small for an engineering application of the model.

6.4 Comparison with Measured Results in Unirradiated Zircaloy-2

Creep and tensile tests were performed on unirradiated zircaloy-2 tubing at room temperature and 382°C. The tests were made at various σ_θ/σ_z ratios to determine the R and P values. The room temperature tests were uniaxial tensile tests and open ended internally pressurized tests. The 382°C creep tests were run for 400 hr at a stress of 120 MPa by internally pressurizing tubing and applying a dead weight to obtain σ_θ/σ_z stress ratios of 2 and 1. The secondary strain was measured in these tests. The room temperature tests gave values for R and P of 2.1 and 4.3, respectively. The 382°C creep tests gave an R of 1.19 and a P of 0.38. These results indicate that different contractile strain ratios apply for irradiation creep and for thermal creep.

7 SUMMARY

A calculation procedure was developed to determine the R and P contractile strain ratios for irradiation induced creep of stress-relieved Zircaloy-2 cladding in BWR's. Values of R and P were derived from the measured diametral and axial deformation data from irradiated BWR assemblies and rods.

A sensitivity study was performed to determine the effects of measurement uncertainty on contractile strain ratio calculation. The uncertainty in water rod growth data had the largest effect, and the uncertainty in spacer spring force had the second largest offset. The measurement uncertainties appear insignificant for an engineering application of the model and for the prediction of in-reactor rod growth and creep down.

The R and P ratios calculated from the post-irradiation deformation data were compared with those determined from tensile tests and creep tests of unirradiated cladding. The comparison indicated that thermal- and irradiation-induced creep have different contractile strain ratios.

REFERENCES

Murty,K.L. and Adams,B.L. (1985) Biaxial Creep of Textured Zircaloy I: Experimental and Phenomenological Descriptions, Mat. Sci. and Eng. 70 169.

Gittus,J.H., Howl,D.A., and Hughes,H. (1970) Theoretical Analysis of Cladding Stress and Strains Produced by Expansion of Cracked Fuel Pellets, Nucl. Appl. and Technol. 9 40.

Franklin,D.G., Lucas,G.E., Bement,A.L. (1983) Creep of Zirconium Alloys in Nuclear Reactor, STP 815, American Society For Testing and Materials, Philadelphia.